



## Design of a Reconfigurable 5-Fingers Shaped Microstrip Patch Antenna by Artificial Neural Networks

<sup>1</sup>Ashraf Aoad\*, <sup>2</sup>Murat Simsek, <sup>3</sup>Zafer Aydin

<sup>1</sup>Department of Electric and Electronics Engineering, Bahcesehir University, Istanbul, Turkey

<sup>2</sup>Department of Electronics and Telecommunication Engineering, Istanbul Technical University, Istanbul, Turkey

<sup>3</sup>Department of Computer Engineering, Abdullah Gul University, Kayseri, Turkey

---

**Abstract**—This paper designs a reconfigurable 5-fingers microstrip patch antenna using artificial neural networks (ANNs). The particular neural networks selected for this task are the source difference method (SD), multilayer perceptron (MLP), prior knowledge input method (PKI) and difference prior knowledge input method (PKID). Employing fine and coarse models for training the networks enables to develop fast and accurate EM-ANN models. The proposed antenna has four modes of operation, which are controlled by two PIN diode switches with ON/OFF states, and it resonates at multiple frequencies between 2-6 GHz. Simulations demonstrate considerable savings in computational costs as compared to the EM simulation software while maintaining the same level of accuracy as the fine models.

**Keywords**—Artificial neural network, source difference method, multilayer perceptrons, prior knowledge method, difference prior method, reconfigurable microstrip antenna, PIN diodes

---

### I. INTRODUCTION

The reconfigurable microstrip antennas have been considered as complex EM structures comprised of planar patch antennas which can have different switching units such as optical switches, PIN diodes, FETs, and radio frequency microelectromechanical system (RF-MEMS) switches [1]. During recent years, reconfigurable microstrip patch antennas have received increasing attention for their applications in cognitive radio, Multiple Input Multiple Output (MIMO) systems, satellites and other applications in wireless communications[2]. They provide the ability to tune various antenna parameters effectively such as the operating frequency, polarization [3], and radiation pattern in a single antenna[4]. Therefore, it is desirable to use reconfigurable antennas to improve frequency, polarization, and radiation diversity as well as the capacity of the system[5]. Various reconfiguration techniques have been employed for designing reconfigurable antennas. Among those, switching mechanisms (e.g. MEMS switches, PIN diodes, and varactors) have played a major role in achieving frequency and polarization diversity[2][6].

Over the years, several numerical and analytical methods that employ detailed electromagnetic models of active/passive components have been developed for designing antennas. However, these methods come with their own set of limitations such as high computational cost and storage requirements. To overcome these challenges, artificial neural networks (ANNs) have been used as efficient alternatives to conventional methods in RF and microwave modeling[7]. ANNs are network systems inspired from the human brain that learn to generalize from observations through abstraction. They have been massively explored as a solution and an optimization technique for modeling linear-nonlinear input/output connections from corresponding data, and are also used more frequently in a number of RF/microwave applications[8] such as telecommunications[9], microstrip circuit design, biomedical sensing and remote sensing[10]. ANNs have also emerged as parallel [11], fast and adaptable machines for EM microwave modelling, simulation and optimization [12]. The parallel distributed processing and generalization ability allow ANNs to calculate and solve complex problems effectively[11].

Several studies have been carried out for designing antennas using ANNs. PKI and SD methods were applied on microwave components to address the use of prior knowledge for reducing the complexity of input/output relationships[13]. In another study, the coarse model was aligned with the fine model of the antenna through space mapping[14]. Design of circular, rectangular, triangular and different shaped microstrip antennas using MLPs were presented in [11][15][16][17]. A large reconfigurable antenna array controlled with MEMS switch was designed to compute  $S_{11}$ -Parameters using multi-layer perceptron (MLP)[18]. In addition to MLP, other types of neural networks have also been investigated. For instance, a slot-loaded microstrip line feed patch antenna is investigated for triple frequency-band operation using radial basis function (RBF) neural network model[19] and a resonance frequency of a coaxial feed C-slotted microstrip antenna is estimated by MLP and RBF[20]. Despite the efforts that employ neural networks for antenna modeling, studies that compare different neural network approaches for designing antennas controlled by PIN diode switches is limited. In the context of reconfigurable antennas, neural networks are typically used as an optimization technique to activate the switches in order to realize a given reconfiguration state (e.g. resonating at certain frequency bands)[2][21].

In this paper, a novel 5-fingers shaped reconfigurable microstrip patch antenna (R5FSMPA) is designed using neural networks. The reconfiguration states of the antenna are realized by PIN diode switches which are modeled as lumped circuit elements. The following ANN methods are compared: SD[13][22], MLP[11][15], PKI[22][13] and PKID[23], which employ simulation data from fine and/or coarse EM models to obtain the input and the output parameters of the networks. In the case of SD and PKID, the difference between the outputs of the fine and the coarse models is taken as the target output whereas in PKI and also PKID, the two models are incorporated as prior knowledge. The antenna has several attractive features such as reconfigurability, small size, and low cost. This paper handles the increasing requests for the continuing application of ANNs in reconfigurable microstrip antenna design: reduction of model development cost[24] and improving the accuracy which is represented by the normalized mean absolute error(NMAE) between the predicted output and the target of the model.

## II. METHODS

### A. Proposed Geometry

The proposed R5FSMPA is shown in Fig. 1, in which  $L_1$ ,  $L_2$  and  $L_3$  represent the length of the radiating patches with  $L_1$  and  $L_2$  mirrored to the opposite side.  $W_1$  (3.3 cm) represents the width of the radiating patch,  $W_2$  (0.3 cm) is the width of patches that correspond to  $L_1$ ,  $L_2$  and  $L_3$ , and  $W_3$  (0.15 cm) represents the unfilled space that includes the two PIN diodes ( $D_1$  and  $D_2$ ). FR-4 is the material of the substrate with a dielectric constant of 4.3 and a height of 0.2 cm. The feeding coaxial conductor is centered in the middle of  $L_3$  with a radius of 0.065 cm. Two different resistors are used to realize the ON and OFF states of the PIN diodes [25]. The large resistor has a resistance value of 1000 Ohm to enable the locking of the DC current on the surface of the  $L_1$  patch when used in the OFF state [26][27]. The small forward resistor has a value of 5 Ohms when used in the ON state [26][27]. For simplicity, the series inductor and parallel capacitor of the lumped elements are neglected in the equivalent circuit model [28].

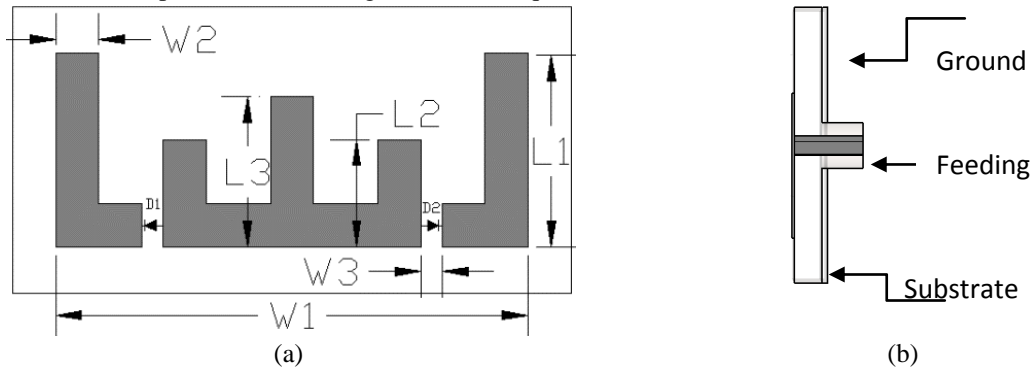


Fig.1 (a) Top view and (b) Side view of the proposed R5FSMPA.  $L_1$ ,  $L_2$  and  $L_3$  are the length parameters,  $W_1$  and  $W_2$  are the width parameters,  $W_3$  is the width of the unfilled space that includes PIN diodes  $D_1$  and  $D_2$

Table 1 shows representative values for the minimum, maximum and mid-point values of  $L_1$ ,  $L_2$ ,  $L_3$ ,  $D_1$  and  $D_2$ , which are among the input features of the neural networks. Other parameters that are shown in Fig. 1 such as  $W_1$ ,  $W_2$ ,  $W_3$ , the radius of the feeding conductor, the thicknesses of radiating patches, substrate and ground are not included in this table because they are not chosen as input parameters.

Table 1: representative values for minimum, maximum and middle points of the length and resistance parameters

Parameter	Symbol	Minimum	Mid-point	Maximum
Longer patch	$L_1$ (cm)	1.2825	1.35	1.4175
Smaller patch	$L_2$ (cm)	0.7125	0.75	0.7875
Mid patch	$L_3$ (cm)	0.9975	1.05	1.1025
ON state	$D_1$ or $D_2 = R_{ON}$ ( $\Omega$ )	-	5	-
OF state	$D_1$ or $D_2 = R_{OFF}$ ( $\Omega$ )	-	1000	-

To obtain the mid-point, minimum and maximum values of the length parameters, the mid-point values (denoted as  $L_i^{mid}$   $i = 1, 2, 3$ ) are first sampled by the EM-simulator. Then the minimum and maximum values ( $L_i^{min}$  and  $L_i^{max}$ ) are computed as formulated in Eq. 11, 22.

$$L_i^{max} = 1.05L_i^{mid} \quad 1$$

$$L_i^{min} = 0.95L_i^{mid} \tag{2}$$

In the next step, equidistant samples are chosen for each length parameter within the interval  $[L_i^{min}, L_i^{max}]$ . For instance, when 4 parameter samples are selected,  $[L_i^{min}, L_i^{max}]$  is divided into 3 equalbins. The following equations formulate how the parameter samples are computed:

$$\Delta_i^k = \frac{L_i^{max} - L_i^{min}}{k - 1} \tag{3}$$

$$L_{ij}^k = L_i^{min} + (j - 1)\Delta_i^k \tag{4}$$

where  $k$  is the total number of parameter samples, which takes integer values from 3 to 5,  $L_{ij}^k$  is the  $j^{th}$  sample value for the  $i^{th}$  parameter with  $1 \leq j \leq k$ , and  $\Delta_i^k$  is the size of each bin. After choosing  $k$  values for each length parameter, a dataset is formed by considering all possible combinations of the parameter values together with the frequency samples from the EM simulator. Since  $k$  can take three possible values, a total of three datasets are generated, which are used to train the neural network models developed in this work. The number of data samples in each of these datasets can be computed according to the following equation:

$$N_{tr}^k = F_s \prod_{i=1}^3 |L_i| \prod_{j=1}^2 |D_j| \tag{5}$$

where  $N_{tr}^k$  is the number of training set samples for a given  $k$ ,  $F_s$  is the number of frequency samples obtained from the EM simulator (which is equal to 200 in this paper),  $|L_i|$  is the number of samples generated for parameter  $L_i$  and  $|D_j|$  represents the number of samples for diode parameter  $D_j$ . For instance, when  $k = 3$  the number of training set samples becomes  $200 \times 3 \times 3 \times 3 \times 1 \times 1 = 5400$ .

### B. Meshing for Fine and Coarse Models

In this paper, the mesh density of the fine model is chosen as 20 lines per wavelength and the total number of mesh cells is 117,600. This requires significant amount of simulation time to compute the results of the fine model as tabulated in

Table 2: The Number Of Samples For Each Parameter, Number of Frequency Samples, Mesh Density Per Wavelength, Number Of Mesh Cells And Simulation Time of Em-Cst For Fine And Coarse Models. The Values Are Obtained And Shown When The Pin Diodes Are In On-On State. (H: Hour, M: Minute, S: Second)

Table 2. For the coarse model, the mesh density is chosen as 12 lines per wavelength and the number of mesh cells is 42,636. Although the simulation time of the coarse model is less than the fine model [14], it could still be regarded as high considering the requirement for repeated runs during the design stage. For both models, the mesh topology must remain unchanged throughout the optimization in order to keep the response of the coarse and the fine models stable and consistent with the design stage [14], which requires taking samples for parameters. Simulations are performed by CST Microwave Studio in Time Domain (TM) using a hexahedral mesh [29] on a computer system with: Core I7 CPU 2.2 GHz and 6 GB RAM. CST uses the Finite Integration Technique (FIT) to calculate the S-parameters for both models [29].

Table 2: The Number Of Samples For Each Parameter, Number of Frequency Samples, Mesh Density Per Wavelength, Number Of Mesh Cells And Simulation Time of Em-Cst For Fine And Coarse Models. The Values Are Obtained And Shown When The Pin Diodes Are In On-On State. (H: Hour, M: Minute, S: Second)

Model	Parameter Samples	Frequency Samples	Mesh density/ wavelength	Mesh Cells	Simulation Time
Fine	3	200	20	117,600	0h 22m 54s
	4	200	20	117,600	0h 50m 52s
	5	200	20	117,600	1h 43m 39s
Coarse	3	200	12	42,636	0h 15m 51s
	4	200	12	42,636	0h 37m 31s
	5	200	12	42,636	1h 13m 37s

### C. Neural Network Modeling

1) *Feed-Forward Neural Network*: In this section, various ANNs are described which are utilized for RF/microwave modeling and design [3][22]. All methods use the same feed-forward architecture also known as multi-layer perceptron (MLP), which consists of an input layer, an output layer and three hidden layers with 20 neurons in each hidden layer. This type of architecture allows the modeling of complex input-output relations in the data [30]. Each layer contains a number of neurons called processing elements. A large number of neurons in the hidden layer give the network

more flexibility, especially if the network has more parameters to optimize[31]. There are also the interconnections between neurons called links. Every link has a weight parameter  $w_j$  associated with it, and the network typically learns these weights from the available training data[32]. Each neuron receives data from neighboring neurons at the previous layer and computes a weighted sum, which is sent to an activation function to produce an output for that neuron. As a result of these operations, the input vector  $\mathbf{x} = [x_1, x_2, x_3, \dots, x_n]^T$  presented to the input layer is fed through the neural network yielding the output vector  $\mathbf{y} = [y_1, y_2, y_3, \dots, y_m]^T$ . The relationship between the input and the output vectors can be represented as

$$\mathbf{y} = f(\mathbf{x}) \quad 6$$

In this equation, the function  $f$  could be highly nonlinear [8]. The initialization of the weight parameters  $w_j$  with small random values is a recommended first step of the training process. Then each  $w_j$  is updated iteratively in the negative direction of the gradient of mean error ( $E$ ), until  $E$  becomes sufficiently small.

$$w_j^{k+1} = w_j^k - \eta \frac{\partial E^k}{\partial w_j} \text{ for } j = 1, 2 \dots n \quad 37$$

The parameter  $\eta$  is called the learning rate that controls the step of the weight update after each training sample is presented to the neural network,  $n$  is the number of weights and  $E^k$  is the mean error at the  $k$ -th instant[18].

2) *Error Measures*: The NMAE measure computes the absolute difference between the predicted outputs and target values from the fine model[16] and is used to assess the accuracy of the neural networks. NMAE is quantified as

$$NMAE = \frac{1}{N} \sum_{j=1}^N \left( \frac{|y_j - t_j|}{|t_j|} \right) \quad 48$$

where the  $y_j$  represents the output variable of the neural network,  $t_j$  is the target value obtained from the fine model and  $N$  is the number of the data samples in the test set. Alternatively, the normalized mean absolute relative error (NMARE) measures the difference between the outputs of the coarse and the fine models ( $\mathbf{y}_c - \mathbf{y}_f$ ) obtained from EM simulator and is calculated as

$$NMARE = \frac{1}{K} \sum_{i=1}^K \left( \left| \frac{y_c^i - y_f^i}{y_f^i} \right| \right) \quad 59$$

where  $K$  is the number of the data samples in fine and coarse models. The fine model is an accurate solution that uses a dense mesh satisfying a rigorous convergence criteria with a convergence NMAE close to 5% [33]. The coarse model is a less accurate solution that uses a coarse mesh which normally satisfies relaxed requirements with a convergence NMARE close to 15% [14].

3) *Neural Network Training, Optimization and Testing*: An ANN model requires three sets of data, called training, validation and test. The training data is used to learn the weight parameters of the neural network, validation data is used to optimize certain parameters of the network (e.g. number of hidden layers, number of hidden nodes, etc), and the test data is used to assess the overall generalization performance of the learned model[22]. The validation set is derived by choosing the same middle point values as in training set for  $L_1$  and by selecting new neighboring samples around the middle points of the other parameters while maintaining the minimum and maximum values in Eqs. 1 and 2. The test set is derived similarly where the same middle point values as in training set are used for  $D_1$  and new neighboring samples are generated for the rest of the parameters within the specified intervals[23]. Neighboring samples are obtained based on the equation  $L_i' = L_i \pm S_i$  (except for  $L_1$  in the validation set and  $D_1$  in the test set) where  $S_i$  represents the value of the interval to neighboring samples and  $L_i'$  represents the neighboring samples. For instance, in the validation set,  $S_i$  is chosen to be -0.03 and -0.06, respectively for  $i = 2$  and  $i = 3$ . In the test set, this parameter is set to -0.04 and -0.05, respectively for the same values of  $i$ . This type of selection ensures that the data samples in validation set and test set do not overlap. Once the sample set is defined for each parameter, all possible combinations of these samples are formed for each set combining with the frequency samples of the simulator. Our neural network models are trained by using Levenberg-Marguardt algorithm[31][16], with tangent-sigmoid transfer functions (TFs) in the hidden layers and a purely linear function in the output layer. The training of the model is achieved by setting the learning rate ( $\eta$ ) to 0.01, the performance goal to 0.00001 and momentum coefficient ( $\mu$ ) to 0.9[34]. The regularization coefficient of the network is chosen as 0.4 where an L2-norm regularizer is used [31]. To optimize the configuration of the neural networks, the number of hidden layers and the number of hidden units in each layer is tuned by minimizing the NMAE measure on the validation set for all states of the PIN diodes. For this purpose, a grid of values is selected for the number of hidden layers (1, 2 and 3) and the number of hidden units (10 to 50 with increments of 10 neurons). Higher values for the number of hidden layers were not considered mainly because the improvements in the accuracy were only marginal while the training times increased considerably. At the end of this procedure, the number of hidden layers is found to be 3 and the number of hidden units is selected as 20. For simplicity, the same network configuration is used for other switching states of the PIN diodes as well. During the testing phase, the accuracy of the optimized model is computed on the test set to assess the actual predictive (i.e. generalization) power of the network. The training, validation and testing of the ANN methods is implemented by the Neural Network Toolbox of MATLAB[31]. This toolbox automatically optimizes the number of epochs according to the accuracy on a validation set (separate from the validation set used to optimize the network configuration above). Details of this optimization procedure can be found in [31].

4) *Neural Network Methods*: The main objective of this work is to obtain low NMAE rates on new test data while maintaining a reasonable computational cost. The following sections explain the neural network methods that are implemented in this paper to meet this goal.

4.1 *Source Difference Method (SD)*: The idea is to exploit the existing data in the form of the fine and the coarse models. In feature extraction stage, the difference between the fine and the coarse models obtained from EM simulator is computed for all the samples as  $\Delta y = y_f - y_c$  ( $y_f$  and  $y_c$  are the outputs for the fine and the coarse models respectively) [22]. This difference is used as the target variable of the neural network. The final stage is a hybrid EM-ANN model which consists of the coarse model and trained neural model. The coarse model computes the coarse output  $y_c$  and the trained neural model predicts the difference. For SD modeling, the input layer is fed by a 6-dimensional vector in all switching states of the PIN diodes where the input parameters might vary from one state to another. For instance, in the ON-ON state  $x = [L_1, L_2, L_3, D_1, D_2, f]^T$  where  $D_1 = D_2 = R_{ON}$ ; in ON-OFF state  $x = [L_1, L_2, L_3, D_1, D_2, f]^T$  with  $D_1 = R_{ON}$  and  $D_2 = R_{OFF}$  and in OFF-OFF state  $x = [L_1, L_2, L_3, D_1, D_2, f]^T$  in which  $D_1 = D_2 = R_{OFF}$ .

4.2 *Multilayer Perceptron (MLP)*: In this method an MLP network is trained only for the fine model [11][15]. The input layer is fed by a 6-dimensional vector in all switching states of the PIN diodes in which input parameters are similar to the SD method.

4.3 *Prior Knowledge Input Method (PKI)*: PKI [22][13] consists of a coarse model to represent the available data and a neural network that represents a mapping between the outputs of the coarse and the fine models. The quality here is by adding the inputs of the fine model  $x_f$ , the output of the coarse model  $y_c$  (prior knowledge) as inputs of the neural network, and choosing  $y_f$  as a target, resulting in a simpler input-output relationship as compared to the fine ( $x_f, y_f$ ) model. For PKI modeling, the input layer is fed by a 7-dimensional vector in all switching states of the PIN diodes where the input vector is defined as  $x = [L_1, L_2, L_3, D_1, D_2, f, y_c]^T$ ,  $D_1$  and  $D_2$  are modeled as in SD and MLP methods.

4.4 *Difference Prior Knowledge Input Method (PKID)*: PKID is considered as a combination of SD and PKI [23]. The inputs of the neural networks are ( $x_f, y_c$ ) and the target is the difference between the outputs of the fine and the coarse models, i.e.,  $\Delta y = y_f - y_c$ . In this method, the input parameters are similar to PKI.

### III. RESULTS AND DISCUSSION

In order to compute the performance of the proposed EM-ANN model, simulated results are obtained using the methods described in Subsection 4. A total of three training sets, three test sets and three validation sets are used since the number of parameter samples (i.e.  $k$  in Eqs. 3 and 4) can take three possible values. The number of data samples in each training set is available in Table 2 Table 3. From Eq. Error! Reference source not found.5, the number of samples in validation and test sets becomes  $N_{vt}^k = F_s = 200$  because only one sample for each length and diode parameter is chosen. For simplicity, a total of 200 data samples are generated for each test and validation set as shown in Eq. Error! Reference source not found.5. The neural network models are repeatedly trained 50 times and the mean, the standard deviation and the minimum of the NMAE values of these 50 models are computed on the test sets to investigate the statistical behavior of the randomized network initialization. The NMARE is also calculated, which shows the distance between the fine and coarse models. Three types of comparisons are made: 1) between NMAE and NMARE, 2) between NMAE of the four methods and 3) elapsed time for the simulated and trained models. The two diodes are modeled as lumped circuit elements (i.e. resistors) for all possible switching states.

Table 2

Table 2 Table 3 shows NMARE values for different number of parameter samples, which eventually results in different number of data samples in training set. Table 3 Table 4 summarizes the NMAE statistics (average, standard deviation and minimum over the 50 repeated network training) for each of the neural networks and for three training sets when the switching state of the PIN diodes is set to ON-ON. For the training data with 5400 samples, it is noticed that the NMAE values for the PKID, PKI and SD are higher than the corresponding NMARE values. In the second set data with 12800 samples, the NMAE values for PKI and PKID are lower than NMARE values. In this setting, the NMAE values of SD is not as good as PKI and PKID (i.e., slightly higher than the NMARE in Table 3). When the training sets with 25000 samples is used, it is observed that all three methods (MLP is only trained for the fine model) have lower NMAE than NMARE, which shows the benefit of using a large training set.

Table 23: nmare values of the fine and coarse models for the on-on state

Parameter Samples	# Data Samples	NMARE
3	5400	0.0648
4	12800	0.0643
5	25000	0.0637

According to Table 3 Table 4, the methods are ranked with respect to the NMAE rates as PKID, PKI, SD and MLP when the models are trained with 5400 data samples. When the number of training samples is increased to 12800 and 25000, the NMAEs of PKID, PKI and SD are lower than that of MLP. For the training sets with 5400 and 25000 samples, the method with the smallest NMAE rate is PKID, followed by PKI, SD and MLP. This order is PKI, followed by PKID, SD and MLP when 12800 samples are used during training. For all the training sets, the NMAEs of PKID, PKI and SD

are lower than that of MLP. Moreover, the resonant frequencies are dual at 3.03 GHz and 5.31 GHz with a return loss of -25.85 dB and -21.87 respectively. For a target return loss of  $S_{11} \leq -10$  dB, bandwidths are 0.355 GHz and 1.27 GHz, respectively as shown in Fig.2Fig.2.

Table 34: Error measures of the ann methods in the on-on state. Each neural network is re-trained 50 times to estimate the nmae statistics

Parameter Samples	# Data Samples	NMAE Statistics	MLP	SD	PKI	PKID
3	5400	Average NMAE	3.308	0.5004	0.2678	0.2031
		Standard deviation	1.968	0.2942	0.2324	0.2187
		Minimum NMAE	0.6965	0.1078	0.0353	0.0322
4	12800	Average NMAE	0.5038	0.0836	0.0181	0.0197
		Standard deviation	0.4899	0.0479	0.0033	0.0105
		Minimum NMAE	0.0169	0.0156	0.0119	0.0101
5	25000	Average NMAE	0.1551	0.0419	0.0188	0.0184
		Standard deviation	0.2682	0.0351	0.0041	0.0083
		Minimum NMAE	0.0183	0.0134	0.0138	0.0124

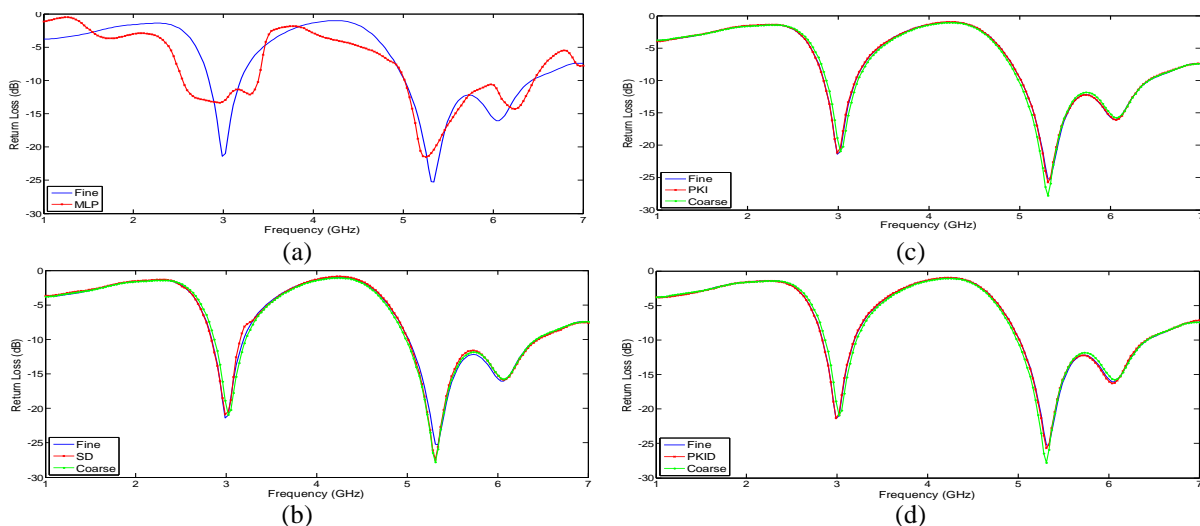


Fig.2  $S_{11}$ -parameter(return loss) of fine model, coarse model and ANN in ON-ON state for the data with 25000 samples (a) MLP, (b) SD, (c) PKI and (d) PKID

Table 4Table5 and .

Table 5Table6 demonstrate the NMAREand NMAE results, respectively for the ON-OFF state of the PIN diodes. For the training set with 5400 samples all three methods have higher NMAE than NMARE. In the second data set with 12800 samples, NAME values of PKI and PKID are smaller than NAMRE, while SD is slightly higher than the NMARE. In last training data set that contains 25000 samples, all methods have lower NMAEas compared to NMARE.

Table 45: nmare values of the fine and coarse models for the on-off state

Parameter Samples	# Data Samples	NMARE
3	5400	0.0434
4	12800	0.0422
5	25000	0.0418

Table 5Table6shows that for the training data set with 5400 samples, the method with the smallestNMAE value is PKID followed by PKI, SD and MLP. For the training data set with 12800 samples, the method with the smallest NMAE rate is PKI followed by PKID, SD and MLP. These methods are ranked with respect to the NMAE rates as PKI, PKID, SD and MLP when the training set contains 25000 samples. For all the training sets, the NMAEs of PKID, PKI and SD

are lower than that of MLP. Moreover, the resonant frequencies are also dual at 2.17 GHz and 5.31 GHz with a return loss of -20.93dB and -25.8 respectively. For a target return loss of  $S_{11} \leq -10$  dB, bandwidths are obtained as 0.28 GHz and 1.2 GHz respectively, as shown in Fig.3Fig. 3.

Table 56: Error Measures Of The Ann Methods In The On-Off State. Each Neural Network Is Re-Trained 50 Times To Estimate The Nmae Statistics

Parameter Samples	# Data Samples	NMAE Statistics	MLP	SD	PKI	PKID
3	5400	Average NMAE	3.467	0.2060	0.1766	0.1139
		Standard deviation	2.151	0.1692	0.1358	0.1144
		Minimum NMAE	0.5933	0.0361	0.0374	0.0264
4	12800	Average NMAE	0.5043	0.0514	0.0210	0.0272
		Standard deviation	0.4533	0.0244	0.0097	0.0169
		Minimum NMAE	0.0211	0.0207	0.0097	0.0098
5	25000	Average NMAE	0.1562	0.0400	0.0184	0.0195
		Standard deviation	0.2203	0.0214	0.0031	0.0077
		Minimum NMAE	0.0195	0.0187	0.0139	0.0133

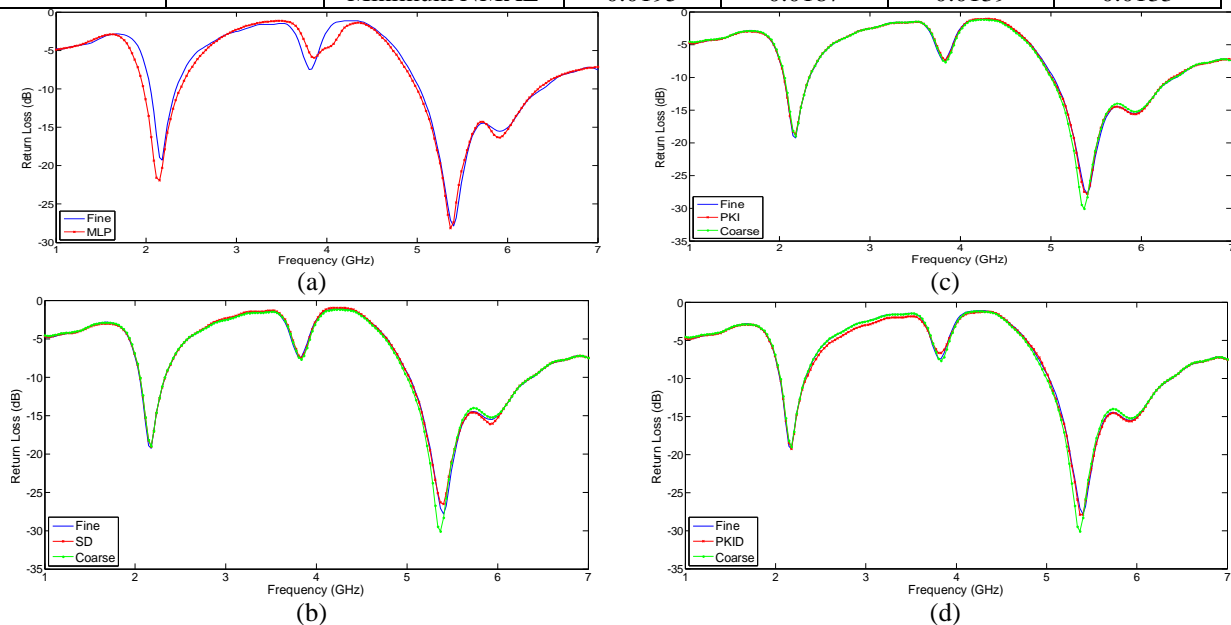


Fig.3  $S_{11}$ -parameter(return loss) of fine model, coarse model and ANN in the ON-OFF state for the data with 25000 samples (a) MLP, (b) SD, (c) PKI and (d) PKID

Table 6 Table 7 and

Table 7

Table 7 Table 8 summarize the NMARE and NMAE results, respectively when the PIN diodes are set to the OFF-OFF state. The results are similar to those obtained in the ON-ON state for the training data with 5400 samples where the NMAE values of the three methods are higher than the NMARE values. When the number of training examples is higher, only the PKI method has an NMAE lower than the corresponding NMARE. The other methods require additional samples to satisfy this condition.

Table 67: nmare values of the fine and coarse models for the off-off state

Parameter Samples	# Data Samples	NMARE
3	5400	0.0374
4	12800	0.0375
5	25000	0.0371

Table 7 Table 8 shows that for the training data set with 5400 samples, methods are ranked with respect to the average NMAE rates as PKID, SD, PKI, and MLP. For the training set with 12800 samples, this ranking is PKI, PKID, SD and MLP, and for the training set with 25000 samples, PKI has the smallest NMAE followed by SD, PKID and MLP. Therefore, in the OFF-OFF state, in which  $D_1$  and  $D_2$  are set to 1000 Ohms, the NMAE rate of MLP is reduced and that of PKID is slightly increased when a large number of training samples is available. This type of behavior is not observed for

PKI and SD. Moreover, in this state the resonant frequency is at 5.5 GHz with a return loss of -30.12 dB. For a target of return loss of  $S_{11} \leq -10$  dB, bandwidth is 1.06 GHz, as shown in Fig. 4. These results are due to isolation of the patches from the radiating body by setting  $D_1 = D_2 = R_{OFF}$ .

Table 78: Error Measures Of The Ann Methods In The Off-Off State. Each Neural Network Is Re-Trained 50 Times To Estimate The Nmae Statistics

Parameter Samples	# Data Samples	NMAE Statistics	MLP	SD	PKI	PKID
3	5400	Average NMAE	3.164	0.1527	0.3685	0.1332
		Standard deviation	3.295	0.2375	0.3279	0.1564
		Minimum NMAE	0.2502	0.0206	0.0294	0.0097
4	12800	Average NMAE	0.5000	0.0490	0.0237	0.0483
		Standard deviation	0.5955	0.0174	0.0257	0.0615
		Minimum NMAE	0.0139	0.0228	0.0052	0.0058
5	25000	Average NMAE	0.0746	0.0456	0.0174	0.0703
		Standard deviation	0.1521	0.0256	0.0093	0.3523
		Minimum NMAE	0.0118	0.0107	0.0070	0.0083

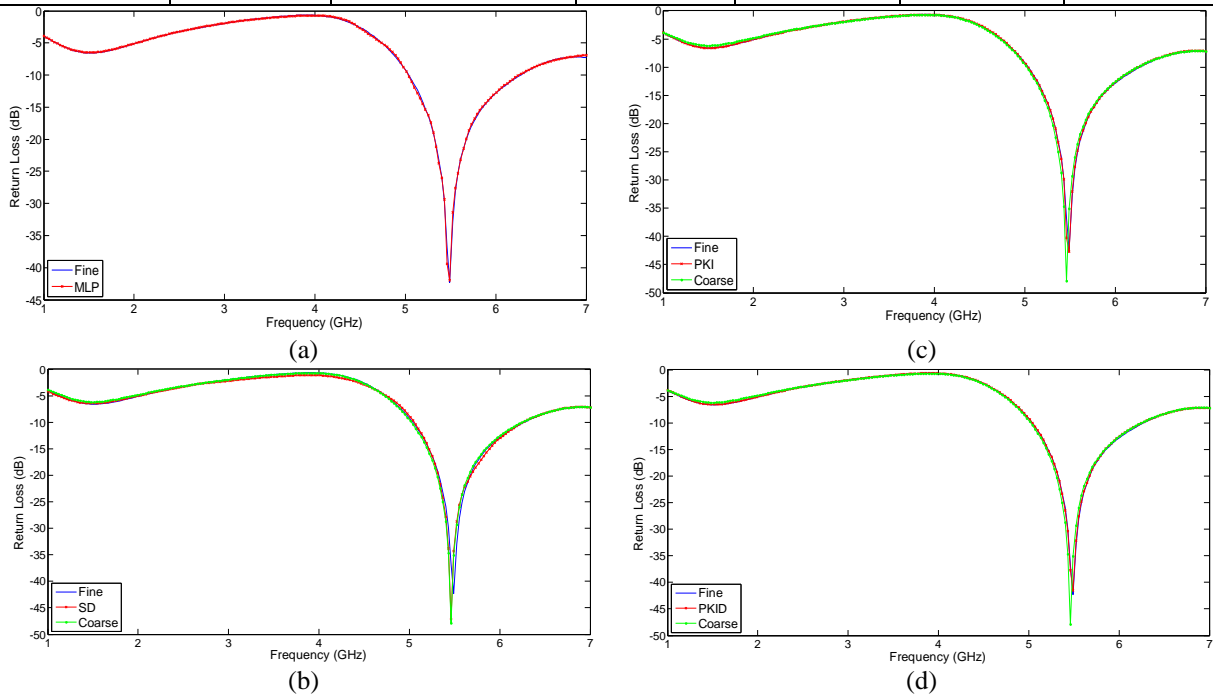


Fig.4  $S_{11}$ -parameter(return loss) of fine model, coarse model and ANN in OFF-OFF state for the data with 25000 samples (a) MLP, (b) SD, (c) PKI and (d)PKID

The methods considered in this work are capable of approximating the fine model with good quality. According to Fig. 2, Fig. 3, Fig. 3, and Fig. 4, the fine EM-model and the predictions of ANNs are in excellent agreement for the training set with 25000 samples except for MLP in the ON-ON state. They are implemented without using any complex antenna formulas [35] but by data generated from the EM simulator. The NMAE and their standard deviations differ from one state to another which reflects the configurability of the antenna. New developed neural network models for different shaped microstrip patch antennas such as Horn shaped and Inverted L [11]. The available error measures are either comparable to the results obtained in this study or higher where the NMAE were reported as 0.0181-0.0745 for an MLP.

The total training and testing times for the fine, coarse and ANN models are tabulated in

Table 8 Table 9. Testing time of the networks is less than one second. The computation time for EM-fine and coarse models is the time spent for obtaining the output  $S_{11}$  and for generating data whereas the time for running ANNs models is the average time spent for training the models 50 times and computing the NMAE on the test set. From these results, it is clearly noticed that the execution times for the models achieved by ANNs bring significant time savings as compared to the EM simulator. Methods are ranked with respect to the execution times (from the smallest to the highest) as PKID,



PKI, MLP and SD in ON-ON state, PKID, SD, PKI and MLP in ON-OFF state and finally PKID, SD, PKI and MLP in OFF-OFF state.

Table 89: Comparison Of Simulation Times For Em-Anns Models In All States For The Data With 25000 Samples

Diode States	EM-Fine	EM-Coarse	MLP (m)	SD (m)	PKI (m)	PKID (m)
ON-ON	1h, 43m,39s	1h,13m,37s	3.122	3.491	2.592	1.918
ON-OFF	1h,59m,09s	1h,20m,57s	4.150	3.104	3.328	2.348
OFF-OFF	1h,39m,29s	1h,14m,40s	3.144	1.884	2.164	1.708

Note that in this paper the results for the OFF-ON state are not reported as they would be the same as the ON-OFF state due to symmetry considerations.

#### IV. CONCLUSION

This study presents a reconfigurable 5-fingers shaped microstrip patch antenna (R5FSMPA), which is modeled by ANN methods. Achieving low error values compared to the error distance between the fine and coarse models indicates that the trained ANN models are accurate for the reconfigurable antenna considered in this work. The results show that compared to SD and MLP, PKID and PKI are in general capable of obtaining low error rates with less training data. It is evident from the comparisons that the results obtained using ANN methods in all states can be much closer to the fine model than the coarse models especially when the number of training samples is sufficiently large. Furthermore, the computation time reduces significantly when ANN methods are used to model the antenna. MLP occupies the last rank in the execution times and the error rates compared to the other methods. The proposed R5FSMPA provides a variety of resonant frequencies such as 3.035 GHz and 5.31 GHz in the ON-ON state, 2.17 GHz and 5.31 GHz in the ON-OFF state, and 5.5 GHz in the OFF-OFF state. As the state of the PIN diodes changes, the resonant frequency shifts toward a lower or a higher frequency. Good bandwidth is also achieved in each switching state. The proposed antenna can be applied to various systems, including wireless communication systems, radar and satellite.

#### ACKNOWLEDGMENT

We would like to thank Assoc. Prof. Neslihan Serap Sengor from Istanbul Technical University and Assoc. Prof. Erdal Korkmaz from Fatih University for their valuable support in this project.

#### REFERENCES

- [1] J. T. Bernhard, *Reconfigurable Antennas*, Champaign: Morgan & Claypool Publishers, 2007.
- [2] J. Costantine, *Design, Optimization and Analysis of Reconfigurable Antennas*, Albuquerque, New Mexico: PhD, 2009.
- [3] A. Zohur, A. Molidevi, D. Rodrigo, M. Unlu, L. Jofre and B. A. Centiner, "RF MEMS Reconfigurable Two-Band Antenna," *IEEE Antenna and Wireless Propagation*, vol. 12, 2013.
- [4] M. F. Ismail, M. K. A. Rahim and H. A. Majid, "The Investigation of PIN Diode Switch on Reconfigurable Antenna," *IEEE International RF and Microwave Conference*, 12th-14th December 2011.
- [5] J. S. Kulandai Raj, J. Bonney, P. Herrero and J. Schoebel, "A Reconfigurable Antenna for MIMO Application," *IEEE Loughborough Antenna & Propagation Conference*, 16-17 November 2009.
- [6] N. Haider, "Recent Developments in Reconfigurable and Multiband Antenna Technology," *International Journal of Antennas and Propagation*, vol. 2013, p. 14, 2013.
- [7] Q.-J. Zhang, K. C. Gupta and V. K. Devabhaktuni, "Artificial Neural Networks for RF and microwave Design-From Theory to Practice," *IEEE Transaction on microwave theory and techniques*, vol. 51, no. 4, pp. 1339-1350, APRIL 2003.
- [8] Q.-J. Zhang and G. L. Creech, "Application of Artificial Neural Networks to RF and Microwave Design," *International Journal of RF and Microwave Computer-Aided Engineering*, vol. 9, no. 3, May 1999.
- [9] B. S. Cooper, "Selected Applications of Neural Networks in Telecommunication Systems," *Australian Telecommunication Research*, vol. 28, no. 2, pp. 9-29, 1994.
- [10] S. P. Gangwar, *ANN Modeling for the Resonance Frequency of Circular Microstrip Antenna*, LAP LAMBERT Academic Publishing, 2012.
- [11] D. K. Neog, *Microstrip Antenna and Artificial Neural Network's Basics, Design and Applications*, Saarbrücken: LAP LAMBERT Academic Publishing GmbH & Co. KG, 2010.
- [12] V. V. Thakare and P. Singhal, "Neural network based CAD model for the design of rectangular patch antennas," *Journal of Engineering Technology Research*, no. 2, pp. 126-129, July 2010.
- [13] P. Watson, K. Gupta and R. Mahajan, "Development of Knowledge Based Artificial Neural Network Models for Microwave Components," *IEEE MTT-S Digest*, pp. 9-12, 1998.
- [14] J. Zhu, J. W. Bandler, L. Fellow, N. K. Nikolova and S. Koziel, "Antenna Optimization Through Space Mapping," *IEEE Transaction on Antennas and Propagation*, no. 55, March 2007.
- [15] F. N. d. Santos, S. S. Nascimento, V. F. Rodriguez-Wsquerre and F. G. S. Filho, "Analysis and Design of Microstrip Antennas by Artificial Neural Networks," *IEEE*, pp. 226-230, 2011.
- [16] T. Khan, A. De and M. Uddin, "Prediction of Slot-Size and Inserted Air-Gap for Improving the Performance of Rectangular Microstrip Antennas Using Artificial Neural Networks," *IEEE Antennas and Wireless Propagation Letters*, no. 12, 2013.

- [17] T. Khan and A. De, "Design of Circular/Triangular Patch Microstrip Antennas using a Single Neural Model," IEEE, 2011.
- [18] A. Patnaik, D. Anagnostou, C. G. Christodoulou and J. C. Lyke, "Modeling Frequency reconfigurable Antenna Array Using Neural Networks," Microwave and Optical Technology Letters, vol. 44, pp. 351-354, 2005.
- [19] M. Aneesh, J. A. Ansari, A. Singh, S. S. Sayeed and Kamakshi, "Analysis of Microstrip Line Feed Slot Loaded Patch Antenna Using Artificial Neural Network," Progress In Electromagnetics Research, vol. 58, pp. 35-46, 2014.
- [20] P. S. Roy and S. Chakraborty, "Design of C-Slotted Microstrip Antenna Using Artificial Neural Network Model," IJRET: International Journal of Research in Engineering and Technology, vol. 2, no. 12, pp. 120-124, December 2013.
- [21] A. Patnaik, D. Anagnostou, C. G. Christodoulou\* and J. C. Lyke, "A frequency reconfigurable antenna design using neural networks," in International Symposium, 2005 IEEE, Orissa, India, 2005.
- [22] Q. J. Zhang and K. C. Gupta, Neural Networks for RF and Microwave Design, ARTECH HOUSE, INC, 2000.
- [23] M. Simsek and N. S. Sengor, "A knowledge-based neuromodeling using space mapping technique: Compound space mapping-based neuromodeling," International Journal of Numerical Modelling: Electronic Networks, Devices and Fields, no. 21, p. 133-149, January - April 2008.
- [24] F. Wang and Q.-j. Zhang, "Knowledge-Based Neural Models for Microwave Design," IEEE Transaction on Microwave Theory and Techniques, no. 45, December 1997.
- [25] "Information and Telecommunication Technology Center (ITTC)," [Online]. Available: <http://www.ittc.ku.edu/>.
- [26] I. Bahl, Lumped Elements for RF and microwave Circuits, Boston-Londo: Artech House, 2003.
- [27] T. Song, Y. Lee, D. Ga and J. Choi, "A Polarization Reconfigurable Microstrip Patch Antenna using PIN Diodes," IEEE Microwave Conference Proceedings (APMC), pp. 616-618, Dec 2012.
- [28] A. Khidre, K.-F. Lee, F. Yang and A. Z. Elsherbeni, "Circular Polarization Reconfigurable Wideband E-Shaped Patch Antenna for Wireless Applications," IEEE Transaction on Antenna and Propagation, vol. 2, no. 61, February 2013.
- [29] E. Leroux, L. Sassi and A. Karvonen, "MEMS design using the Finite Integration Technique," MEMSWAVE, 2006. [Online]. Available: <https://www.cst.com>.
- [30] P. M. Watson and K. C. Gupta, "EM-ANN Models for Microstrip Vias and Interconnects in Dataset Circuits," BEE Transactions on Microwave Theory and Techniques, no. 44, December 1996.
- [31] "Neural Network Toolbox," [Online]. Available: <http://www.mathworks.com/help/nnet/index.html>.
- [32] A. K. Jain and K. Mohiuddin, "Artificial Neural Networks:A Tutorial," IEEE, 1996.
- [33] R. J. Pratap, Design and optimization of Microwave Circuits and Systems Using Artificial Intelligence Techniques, Georgia, Atlanta: Georgia Institute of Technology, 2005, p. 21.
- [34] "Neural Network Toolbox," [Online]. Available: <http://www.mathworks.com/help/nnet/ref/traingdm.html>.
- [35] C. Christodoulou and M. Georgiopoulos, Applications of Neural Networks in Electromagnetics, Boston-London: Artech House, 2001.